CHAPTER 13

A Brief Introduction to Voltage-Gated K^+ Channels

Benoît Roux

The University of Chicago, Institute of Molecular Pediatric Sciences,
Gordon Center for Integrative Science, 929 East 57th Street, room W323B, Chicago, IL 60637, USA

I. Introduction
II. Structure of Kv Channels and Gating Mechanisms
  A. Structural Information
  B. Gating Movements, Large or Small?
  C. Common Grounds
III. Free Energy and Membrane Voltage
IV. Conclusion
  References

I. INTRODUCTION

Voltage-gated K^+ (Kv) channels are transmembrane proteins that control and regulate the flow of K^+ ions across cell membranes (Sigworth, 1993; Yellen, 1998; Hille, 2001; Bezanilla *et al.*, 2003). In response to changes in the membrane potential, they undergo conformation changes, thereby allowing or blocking the conduction of ions. Structurally, Kv channels are formed by four subunits surrounding a central aqueous pore for K^+ permeation. Each subunit comprises six transmembrane segments (Tempel *et al.*, 1987), S1–S6, the first four transmembrane segments, S1–S4, constituting the voltage sensor domain, while the last two transmembrane segments, S5 and S6, from each of the four subunits join around a common axis to form a selective ion-conducting pore (Bezanilla, 2000). Positively charged residues along S4, mostly arginines, appear to be mainly responsible for the coupling to the membrane voltage (Papazian *et al.*, 1991; Aggarwal and MacKinnon, 1996; Seoh *et al.*, 1996). Upon membrane depolarization, the voltage sensor in each subunit undergoes voltage-dependent transition from a resting to an activated state, resulting in a conformation that allows the

Current Topics in Membranes, Volume 60
1063-5823/08 $35.00

DOI: 10.1016/S1063-5823(08)00013-6

opening of the (Bezanilla *et al.*, 1994; Zagotta *et al.*, 1994). Once all of the four subunits are in the activated state, opening of the pore gate occurs cooperatively via a concerted transition that is weakly voltage-dependent (Ledwell and Aldrich, 1999). After their opening, the channels start to enter into a non-conductive state via a process that is called slow inactivation.

To understand how Kv channels function, requires knowledge of the structure of the channel in its various states to atomic resolution, and knowledge of how the different parts of the protein change their conformation during voltage-gating. Ultimately, one would like to be able to "visualize", atom-by-atom, how the protein moves as a function of time in response to the membrane potential. Little by little, progress is being made toward this goal. In this brief chapter, I will try to provide a view of the recent progress that has been made in recent years. In the first section, I review the current state of knowledge about the structure of Kv channels.

II. STRUCTURE OF Kv CHANNELS AND GATING MECHANISMS

A. Structural Information

X-ray crystallography of the KvAP channel offered the first view of the molecular architecture of a voltage-activated K^+ channel at atomic resolution (Jiang et al., 2003a, 2003b). Two independent X-ray structures were obtained. They are shown in Fig. 1. The full tetrameric channel was crystallized in complex with a monoclonal Fab antibody fragment bound to the S3–S4 loop. In addition, the isolated voltage sensor, consisting of S1 to S4, was also crystallized, again with a monoclonal Fab antibody bound to the S3–S4 loop. The conformations of the

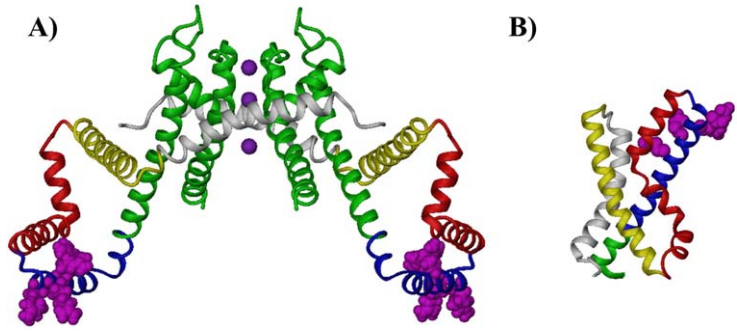

FIGURE 1 Crystallographic structures of the KvAP channel (S1, white; S2, yellow; S3, red; S4, blue; S5–S6 pore, green). (A) Structure of the full length channel is with the four arginine residue in space filling (magenta) is displayed in a transmembrane-like orientation (only two subunits are shown for the sake of clarify). (B) Structure of the isolated voltage sensor S1–S4. (For interpretation of the references to color in this figure legend, the reader is referred to the web version of this book.)

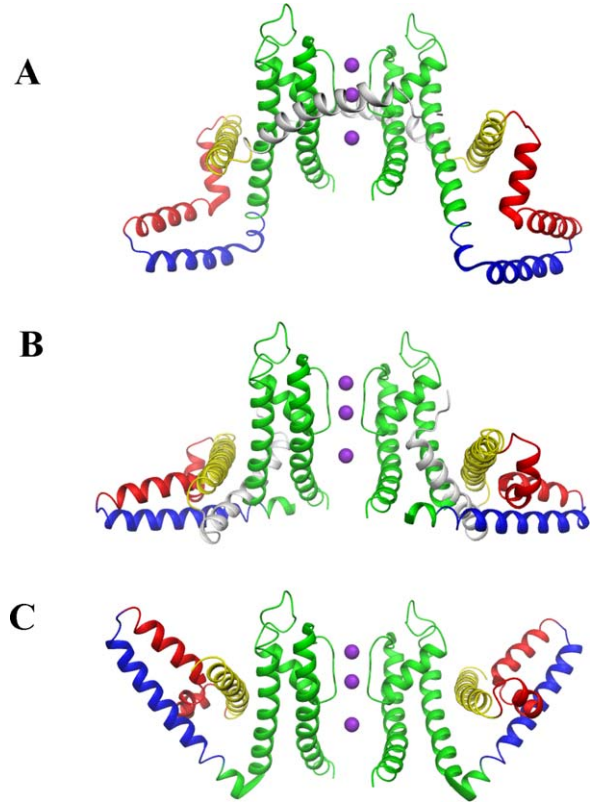

FIGURE 2 Structural models of the KvAP channel from (Jiang et al., 2003a, 2003b). (A) X-ray structure of the full-length KvAP channel viewed from the side with the intracellular solution below. (B) Identical view with the X-ray structure of the isolated voltage sensor (S1–S4) docked according to the position of S2 in the X-ray structure of the full-length channel (obtained by superposing the backbone of S2 from the two X-ray structures as described in (Jiang et al., 2003a, 2003b). (C) Representation of the modeled open state structure of KvAP based on the paddle depth and orientation as described in (Jiang et al., 2003a, 2003b).

voltage-sensor in the two X-ray structures are quite different (Fig. 1). Recognizing that the structure of the full channel was not entirely consistent with the expected architecture of the functional channel based on numerous experimental results, the authors concluded that the X-ray structure was probably distorted. Occurrence of such a non-native conformation in protein crystallography is unusual, but in this case may have been caused by the combined effect of the detergent and the interaction of the Fab fragment. To circumvent the problems with the distorted X-ray structure, the authors used the structure of the isolated voltage sensor and accessibility data from trapping experiments of biotinylated channels by avidin to

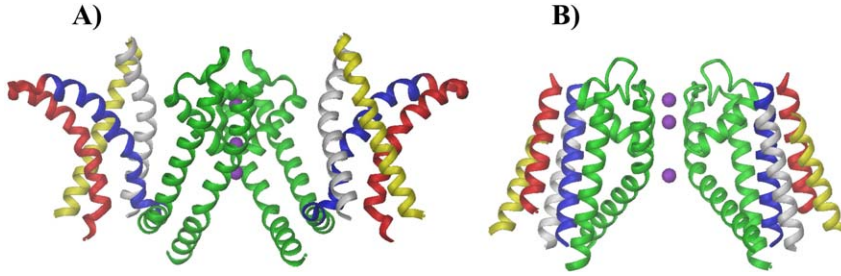

FIGURE 3 Comparison of the crystallographic structure of the Kv1.2 channel (Long *et al.*, 2005) with the approximate model of the Shaker channel in the open state from (Laine *et al.*, 2003) build from the X-ray structure of the MthK channel (Jiang *et al.*, 2002).

construct models of the channel in the open and closed states (Jiang et al., 2003a, 2003b). Those models were generated as shown in Fig. 2, by superimposing the S2 helix from the full length channel and the isolated voltage sensor. This modeling is suggestive of the basic feature of the "up-down" movement characteristic of the paddle model. At the time, the resulting model of KvAP in an open state differed extensively with an approximate model of the *Shaker* channel based on a wide range of experimental data (Laine *et al.*, 2003, 2004). The controversy about the structure of Kv channels then reached a maximum (Cohen *et al.*, 2003; Laine *et al.*, 2004). The crystal structure of Kv1.2 from rat brain provided the first atomic resolution view of a voltage-gated potassium channel in a native conformation (Long *et al.*, 2005) has considerably clarified these matters. According to the experimental conditions, the crystallographic structure of Kv1.2 should correspond to a channel with its voltage-sensors near an their activated position.

As shown in Figs. 3 and 4, the overall topological features of the X-ray structure of Kv1.2 are in excellent accord with a model of *Shaker* K^+ channel in its activated open state deduced on the basis of a wide range of structural, functional and biophysical experiments. Namely, the voltage sensor is formed by a bundle of four anti-parallel transmembrane α-helices, S1–S4, each with their N- and C-terminal ends exposed alternatively to the intra and extracellular solution. Seen from the extracellular side, the S1–S4 helices of the voltage sensor are packed in a counterclockwise fashion, and the S4 helix of a subunit is making contact with the S5 helix of the adjacent subunit in the clockwise direction (Laine *et al.*, 2003). This is displayed in Fig. 4. The excellent accord between the X-ray structure and results from numerous functional and previous models deduced from a wide range of biophysical experiments considerably strengthens the consensus about voltage-gated K^+ channels. It is now apparent that the broad features of the model of the *Shaker* channel in the open state based on all available data at the time and the open-state X-ray structure of the MthK channel (Jiang *et al.*, 2002) was much closer to the X-ray structure of the Kv1.2 channel than the models presented by (Jiang et al., 2003a, 2003b), where the S4 segment was located at the

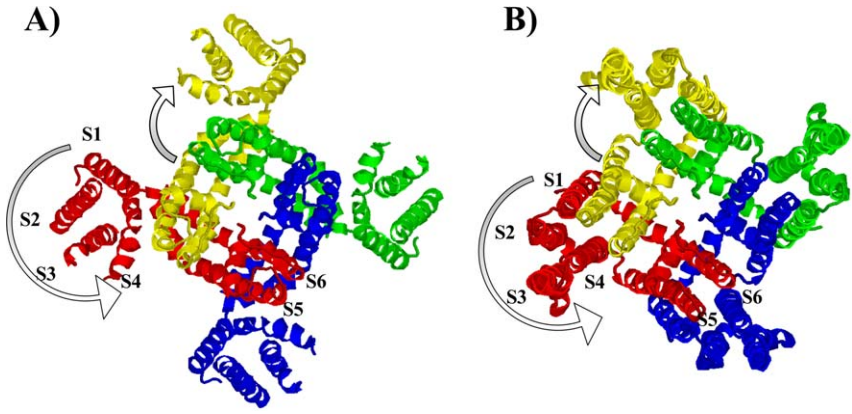

FIGURE 4 Comparison of the X-ray structure of the Kv1.2 channel seen from the extracellular side (Long *et al.*, 2005) with the approximate model of *Shaker* in the open state from (Chanda *et al.*, 2005). As previously established in (Laine *et al.*, 2003), the four transmembrane helices of the voltage sensor are packed in a counterclockwise direction, and the voltage sensor from one subunit is within proximity of the pore domain from the adjacent subunit in the clockwise direction.

periphery of the protein and the S2 was close to the pore. The good agreement also validates the general strategy for translating available experimental data into structural models. Additional efforts incorporating also the information from the X-ray structure of the KvAP channel together with available experimental data led to better models of the *Shaker* K^+ channel in the open and the closed state (Chanda *et al.*, 2005). Though there clearly some structural differences, the main structural features of the open state model are in are in excellent agreement with the X-ray structure of the Kv1.2 channel (Long *et al.*, 2005).

An interesting feature of the X-ray structure is the modular nature of the voltage sensor domain and its lack of extensive interactions with the pore domain. About 66% of molecular surface of the transmembrane region of each voltage-sensor S1–S4 is exposed to lipids. The existence of nearly independent voltage-sensing modules is consistent with the functional chimeras engineered by substituting the pore domain of the KcsA channel into the voltage-gated Shaker channel (Lu *et al.*, 2001) and naturally compatible with the allosteric model of channel gating developed by Aldrich and co-workers (Ledwell and Aldrich, 1999). Furthermore, the discovery of voltage-sensors-like domains with high sequence similarity to the S1–S4 helices in two unrelated membrane-associated proteins lacking any channel-like central pore domain (Murata *et al.*, 2005; Okamura *et al.*, 2006; Ramsey *et al.*, 2006) reinforced the concept of the S1–S4 helical bundle as independent functional modules. This suggests that biophysical experiments performed on isolated voltage-sensors may be able to reveal some of the universal features of gating motions, without the complicated coupling to the pore domain.

While there is now a broad agreement concerning the open (activated) conformation of Kv channels, there is no apparent consensus concerning the magnitude and the character of the motion underlying voltage gating. Three principal models of the conformational change of the voltage-sensing domain have been proposed: the sliding helical screw model (Catterall, 1988), the paddle model (Jiang et al., 2003a, 2003b), and the transporter model (Chanda *et al.*, 2005). The helical screw model is most closely associated with the most traditional view of voltage-gating (Catterall, 1988). It pictures the S4 helix as being completely enclosed inside a gating pore formed by the rest of the protein in which it could slide up and down during gating. The paddle model describes the gating process as a whole body translocation of the S3–S4 helix-turn-helix through the lipids (Jiang et al., 2003a, 2003b). While both the sliding helical screw and the paddle model posit a substantial translocation of the S4 segment, the transporter model invokes smaller movements (Chanda *et al.*, 2005). This model pictures the coupling to the transmembrane voltage through small movements of the charged residues of the voltage sensor across a transmembrane electric field focused by high dielectric aqueous crevices.

B. Gating Movements, Large or Small?

Arguments about "large" versus "small" movements within the voltage sensing domain now appear to be at the heart of the controversy concerning the mechanism of voltage-gating. To make matters worse, there exist experimental data supporting both large and small movements and this certainly contributes to create confusion. Luminescence resonance energy transfert (LRET) experiments for a fluorophore attached to various parts of the voltage–sensor (Cha *et al.*, 1999; Posson *et al.*, 2005), fluorescence transfer to the hydrophobic anion dypicrylamine (DPA) localized at the lipid–aqueous intersurface (Chanda *et al.*, 2005), and kinetic analysis of inhibitory toxin binding to the voltage sensor (Phillips *et al.*, 2005), all seem to be consistent with small (1–2 Å) movements upon channel gating. In contrast, trapping experiments of biotinylated channels by avidin seem to indicate rather large (15–20 Å) movements of the S3–S4 helices (Jiang et al., 2003a, 2003b; Ruta *et al.*, 2005). In many ways, the controversy about the magnitude and character of the movement underlying voltage gating reflects the uncertainty of the various experimental methods and the limited information about the conformation of the resting (closed) state.

The difficulty in interpreting the various results in terms of a well-defined movement is illustrated schematically in Fig. 5 for three types of experiments, LRET (Posson *et al.*, 2005), hannatoxin inhibition (Phillips *et al.*, 2005), and biotin–avidin trapping experiments (Ruta *et al.*, 2005). For example, LRET experiments use the rate of fluorescence energy transfer as a spectroscopic ruler by estimating the donor–acceptor distance according to Förster theory (Posson *et al.*,

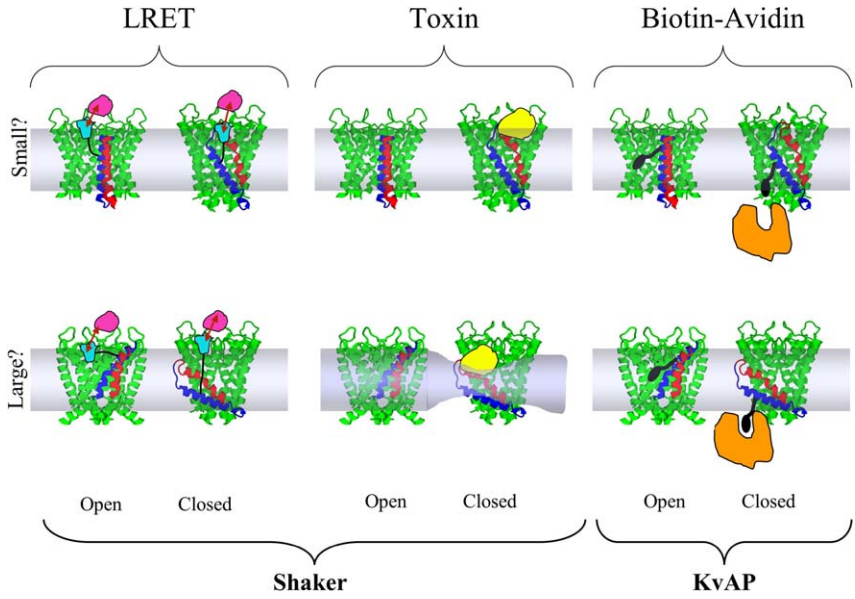

FIGURE 5 Schematic illustration of the possible interpretation as "large" or "small" movements from three methods commonly used to determine the magnitude of the movement upon channel gating. The experiments include LRET (Posson *et al.*, 2005), toxin inhibition (Phillips *et al.*, 2005), and biotin–avidin trapping experiments (Ruta *et al.*, 2005).

2005). First, a cysteine is substituted at a specific position in the channel, and then linked to a thiol-reactive terbium chelate to act as the donor. An acceptor is then placed elsewhere in the channel or in a toxin binding bound to the channel. While the energy transfer rate may accurately report the donor–acceptor distance, it is important to keep in mind that the latter is attached to the backbone of the channel via a flexible molecular linker that is 5–10 Å long. As illustrated in Fig. 5, a small observed change in donor–acceptor could be consistent with both a small or relatively large movement within the voltage sensor. In addition, if there are large conformational fluctuations in the donor–acceptor distance, the short values tend to weight more because the Förster energy transfer varies like the inverse 6th power of the donor–acceptor distance (Selvin, 2002). Channel inhibition of *Shaker* channels by hannatoxin from tarantula also provide information about the movement of the voltage sensor upon channel activation (Phillips *et al.*, 2005). This toxin inhibit the movement of the opening of Kv channels by binding to the S3–S4 region of the voltage sensor, keeping it near its resting position. Hanatoxin forms a strong and stable complex with the voltage sensors and its affinity is reduced by voltage-sensor activation, explaining why the toxin stabilizes the resting conformation. The toxin is also known to partition near the membrane–solution interface, which puts a limit on the amount of motion. Consequently, the

S3–S4 region cannot move than the outer half of the bilayer during activation. However, the exact magnitude of the movement depends on assumptions about the local shape and the amount of distortion of the membrane–solution interface in the neighborhood of the voltage sensor (Fig. 5). Finally, the magnitude of the movement has been estimated with trapping experiments of biotinylated KvAP channels by avidin (Jiang et al., 2003a, 2003b; Ruta *et al.*, 2005). In those experiments, a biotin is tethered to the voltage sensor via a cysteine using linkers of different lengths and the closed and open conformations are trapped irreversibly by avidin binding to the biotin from the intra or extracellular solution. Those experiments indicate that the S1 and S2 helices do not move significantly during gating. But movements on the order of 15–20 Å were inferred for the S3–S4 region of the voltage sensor. In interpreting those results, it is important to keep in mind that the binding of biotin with avidin is essentially irreversible. This means that any encounter of biotin with avidin, even through a rare thermal fluctuations, could lead to binding and, thereby, channel inhibition. From this point of view, biotin–avidin trapping experiments provide an upper bound to the magnitude of typical movements that can occur.

Despite the apparent discrepancies, the situation is progressively becoming clearer as more experimental data is accumulated about the closed state. The model of *Shaker* in the closed state assumes an inward vertical movement of ∼4 Å at the level of the first arginine in the S4 helix (Chanda *et al.*, 2005). A refined model of the closed state based on the structure of the Kv1.2 channel using the Rosetta method suggests a similar inward movement of S4 (Yarov-Yarovoy *et al.*, 2006). Such inward displacement is compatible with the LRET measurements, but appears much shorter than the 15–20 Å extracted from the biotin–avidin experiments. However, a careful analysis reveals that the discrepancy with the biotin–avidin experiments is more limited than expected (see also Yarov-Yarovoy *et al.*, 2006). This is illustrated in Fig. 6 using the approximate models from (Chanda *et al.*, 2005), where residues are color-coded according to the accessibility deduced from the biotin–avidin experiment. The main discrepancies, indicated by the colored arrows, are on the order of 5–8 Å. While this is not perfect accord, the biotin–avidin results could be rationalized if the voltage-sensor was undergoing inward–outward thermal fluctuations on the order 3–4 Å. In fact, this seems likely given its high flexibility as indicated by electron paramagnetic resonance (EPR) (Cuello *et al.*, 2004). This means that the "gap" between the extreme views with "small" and "large" movements is not as large as commonly thought.

Recently, the approximate model of *Shaker* in the closed state from (Chanda *et al.*, 2005) was used as a template to guide a search for possible cross-links between S4 and other parts of the voltage sensor (Campos *et al.*, 2007). In qualitative agreement with the model, experiments with substituted cysteine residues in *Shaker* showed that, at hyperpolarized potentials, both I241C (in S1) and I287C (in S2) can spontaneously form disulfide and metal bridges with R362C, the

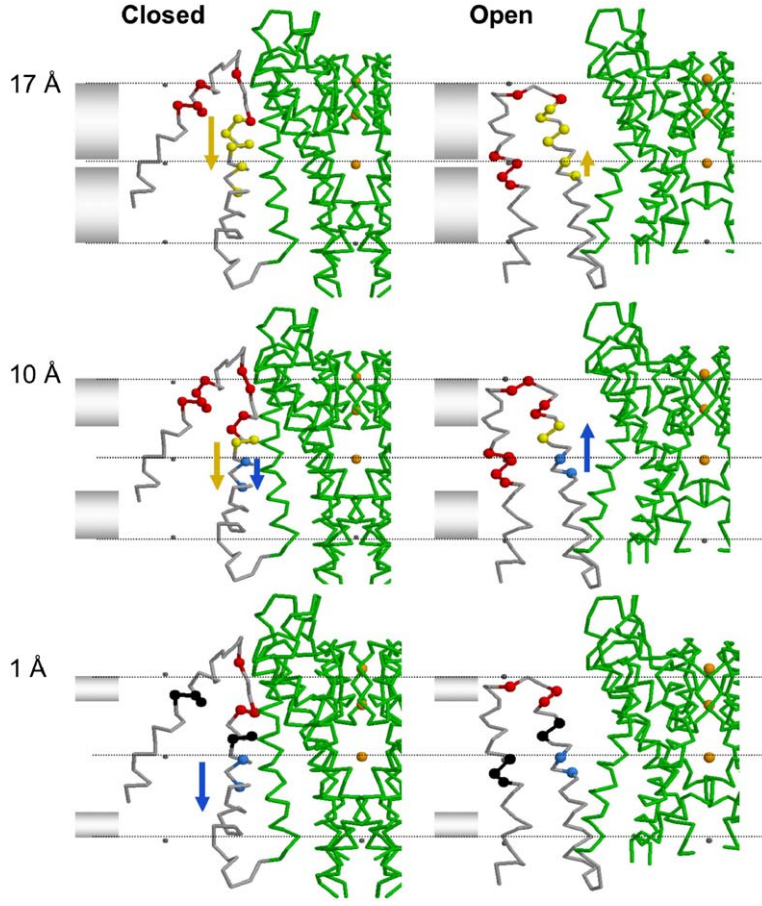

FIGURE 6 Comparison of the approximate open and closed models of *Shaker* from (Chanda *et al.*, 2005) to the biotin–avidin trapping experimental data (Ruta *et al.*, 2005). The color code indicates the residues accessible only from the extracellular side (red), the residues accessible only from the intracellular side (blue), the residues accessible only from both side (yellow), and the residues that are inaccessible from either side (black). The grey slab area indicate the accessible depth with the different length of biotin linkers (17, 10 and 1 Å) and the colored arrows indicate the discrepancies between the models and the biotin–avidin trapping data. (For interpretation of the references to color in this figure legend, the reader is referred to the web version of this book.)

position of the first charge-carrying residue in S4. These results constrain unambiguously the closed-state positions of the S4 segment with respect to the S1 and S2 segments, which are known to undergo little or no transmembrane (vertical) movement during gating. Remarkably, these results are entirely compatible with a series of mutations yielding a favorable pathway for the rapid conduction

of Na^+ at the center of the voltage sensor in the inactivated ("down") state, the so-called "Omega current" (Tombola *et al.*, 2007). Refined models of the closed states in good accord with all these results have been generated using the Kv1.2 X-ray structure using the Rosetta method (Pathak *et al.*, 2007).

To satisfy these constraints, the S4 segment must undergo an axial rotation of about 180 degree and a vertical movement of about 6 to 8 Å at the level of the first charged residue (R362 in *Shaker*) in going from the open to the closed state of the channel. This further reduces the discrepancy with the biotin–avidin trapping experiments discussed in Fig. 6 (see above). Essentially, the first arginine moves from the membrane–solution interface, as shown in the X-ray structure of the Kv1.2 channel (Long *et al.*, 2005), to the middle of the outer leaflet of the bilayer (Campos *et al.*, 2007). As a result of the rotation, the positively charged residues of S4 point toward the S1–S3 helices in the closed state and no charged residues is directly exposed to the lipid hydrocarbon region in the open state or in the closed state. Models of the closed state suggest that the charged residues of S4 follow an energetically favorable pathway in going from the "up" activated state to the "down" resting state (Tombola *et al.*, 2007; Campos *et al.*, 2007; Pathak *et al.*, 2007).

C. Common Grounds

The emerging picture retains some features of the three main models. The whole body movement of S4 is reminiscent of the traditional helical screw model (Catterall, 1988), the presence of high dielectric crevices contributes to a focused field as in the transporter model (Chanda *et al.*, 2005), and the S4 segment is not moving within a hydrophilic "gating-pore" formed by the protein as emphasized in the paddle model (Jiang et al., 2003a, 2003b). But some specific details of the proposed models begin to be disproved as well. In particular, the magnitude of the movement compatible with the data is 7–8 Å, which is clearly larger than 1–2 Å of the "small movement" camp (Cha *et al.*, 1999), but yet smaller than the 15–20 Å of the "large movement" camp (Jiang et al., 2003a, 2003b; Ruta *et al.*, 2005). The S4 helix is not predominantly surrounded by lipids as initially pictured in the paddle model. In addition, the concept of arginines residues acting as hydrophobic cations that project directly into the nonpolar hydrocarbon core of the membrane (Jiang et al., 2003a, 2003b; Long *et al.*, 2005) does not seem relevant to channel gating, mostly like due to the large free energy for dragging the side chain from water to the membrane interior (Dorairaj and Allen, 2007). This is further supported by molecular dynamics simulations of the Kv1.2 channel in the open state, which shows that the hydration of the voltage sensor is extensive and that the arginine along the S4 segment are not directly exposed directly to the hydrocarbon region of the membrane (Treptow and Tarek, 2006; Jogini and Roux, 2007).

III. FREE ENERGY AND MEMBRANE VOLTAGE

The transmembrane potential affects the configurational equilibrium of membrane-bound proteins, and provide the driving force for activating voltage-gated channels. Assuming only two conformational states, open and closed for the sake of simplicity, the probability of the open state can be expressed in terms of the total free energy as (Sigworth, 1993),

$$P_o = \frac{\exp[-G_o^{tot}/k_B T]}{\exp[-G_o^{tot}/k_B T] + \exp[-G_c^{tot}/k_B T]}.$$

The total free energy of the protein in the open state can be written as the sum of two contributions. The first contribution represents the intrinsic energy of the protein, which is independent of the membrane potential. The second contribution represents the coupling between the protein and the transmembrane potential V_{mp}. This coupling takes the form of an effective state-dependent charge Q multiplying the transmembrane potential V_{mp}. The total free energy of the open state is thus,

$$G_o^{tot} = G_o + Q_o V_{mp}$$

and likewise for the closed state. A simple re-arrangement allows to re-write P_o as,

$$P_o = \frac{\exp[\Delta Q(V_{mp} - V_{1/2})/k_B T]}{1 + \exp[\Delta Q(V_{mp} - V_{1/2})/k_B T]},$$

where $\Delta Q = (Q_c - Q_o)$ and $V_{1/2} = (G_o - G_c)/\Delta Q$. The quantity $V_{1/2}$ corresponds to the voltage at which one half of the population of proteins are in the open state, and one half are in the closed state. It is directly related to the relative free energy of these two states in the absence of an applied voltage. The quantity ΔQ is the "gating charge" (Sigworth, 1993). Kv channels display a large gating charge, on the order of about 12 to 14 elementary charge (Schoppa *et al.*, 1992). In simple terms, channel opening corresponds to the outward translocation of a large positive charge ΔQ. This charge is responsible for the strong coupling of the conformation of the channel to the transmembrane voltage.

It is important to try to reconcile the observed gating charge to the structure. In the simplest case of a perfectly planar membrane, the atomic charges of an intrinsic protein are expected to interact directly with the (constant) transmembrane electric field. In such a case, the gating charge ΔQ would simply be related to the displacement of each atomic charge of the protein in the direction perpendicular to the membrane surface. However, as illustrated in Fig. 7 the situation is more complicated if the surface of the protein is irregular and there are high dielectric aqueous crevices. For instance, there appears to be an aqueous channel-like region at the center of the voltage sensor. Such aqueous pore has been inferred by mutations in S4 that enabled the rapid conduction of ions in the inactivated ("down") state (Starace and Bezanilla, 2004; Tombola *et al.*, 2005, 2007; Campos

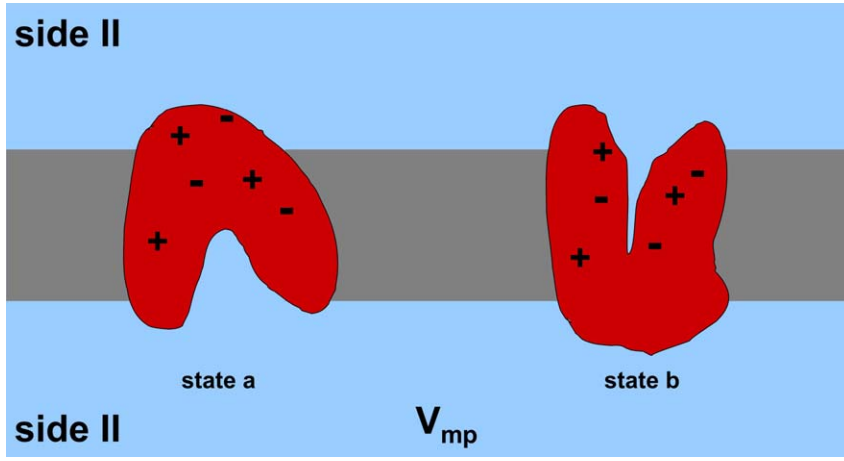

FIGURE 7 Schematic representation of a protein with embedded charges with irregular boundaries with the high dielectric solvent. In such complex geometry, the naïve concept of a constant transmembrane field is not valid.

et al., 2007). For example, conduction of H^+ through the voltage sensor is not normally observed in the case of the wild-type channel, but substitution of R371 by a histidine in *Shaker* (corresponding to R303 in Kv1.2) is sufficient to allow H^+ conduction. The presence of water molecules within the voltage sensor is qualitatively consistent with the concept of high dielectric aqueous crevices suggested previously by Islas and Sigworth (2001) and by Bezanilla and co-workers (Starace and Bezanilla, 2004). As illustrated by continuum electrostatic computations using simple geometries (Islas and Sigworth, 2001; Chanda *et al.*, 2005; Grabe *et al.*, 2004), a fundamental consequence of such high dielectric regions is to focus the transmembrane potential. To think rationally about those effects, it is necessary to have a theory of voltage gating that can be applied at the atomic level.

An effective theoretical formulation of the membrane potential and its influence on the configurational free energy of an intrinsic protein of arbitrary shape can be derived using macroscopic continuum electrostatics (Roux and Simonson, 1999). Following a Green's function decomposition of the total free energy, we obtained the modified Poisson–Boltzmann (PB) equation to account for the effect of the transmembrane potential (Roux, 1997),

$$\nabla \cdot \left[\varepsilon(\mathbf{r})\nabla\phi_{\mathrm{mp}}(\mathbf{r})\right] - \bar{\kappa}^2(\mathbf{r})\left[\phi_{\mathrm{mp}}(r) - \Theta(\mathbf{r})\right] = 0,$$

where $\varepsilon(\mathbf{r})$ and $\kappa(\mathbf{r})$ are the space-dependent dielectric coefficient and Debye–Hückel ionic screening factor, respectively, and $\Theta(\mathbf{r})$ is a Heaviside step function equal to 0 on the intracellular side of the membrane and equal to 1 on the extracellular side. While the atomic charges of the protein do not appear in the

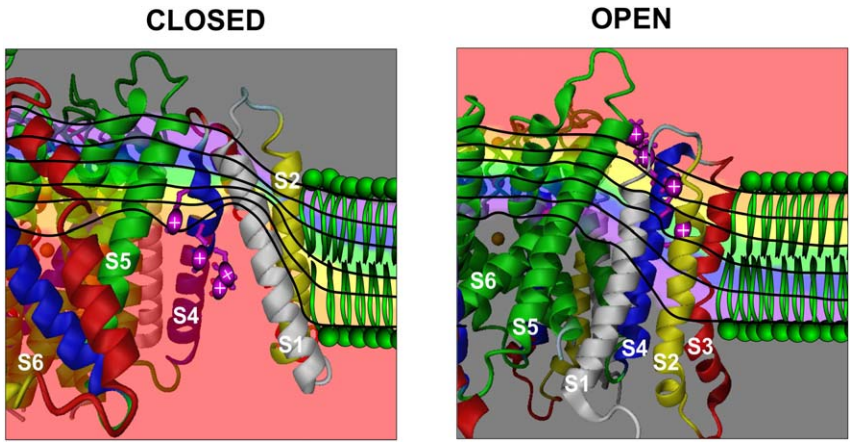

FIGURE 8 The PB-V equation (Roux, 1997) was solved numerically with a finite-difference relaxation algorithm for the approximate model of the Shaker channel in the closed and open states (Chanda *et al.*, 2005). In the calculations, the channel is represented explicitly with atomic details while the membrane is represented as a planar slab of dielectric 2, and the ions and water molecules by a continuum with dielectric constant of 80 and a salt concentration of 150 mM. The transmembrane field is focused and is most intense toward the extracellular half of the membrane.

PB-V equation, its molecular shape is taken into account in constructing the functions $\varepsilon(\mathbf{r})$ and $\kappa(\mathbf{r})$. The gating charge of the channel is then calculated from the ϕ_{m} calculated from the PB-V equation for the both the open and closed states,

$$\Delta Q = \sum_i q_i \left[\phi_{\mathrm{mp}}^{(\mathrm{o})}(\mathbf{r}_i)\right] - \sum_i q_i \left[\phi_{\mathrm{mp}}^{(\mathrm{c})}(\mathbf{r}_i)\right],$$

where q_i are the protein charges and $\mathbf{r}_i$ is their position. Mathematically, $\phi_{\mathrm{mp}}(x, y, z)$ varies between 0 (on the extracellular side) to 1 (on the intracellular side) and corresponds to the dimensionless fraction of the applied transmembrane potential V_{mp} at the point $\mathbf{r}$. To illustrate how the PB-V theory works, we have calculated the gating charge for the approximate models of the open and closed states of the *Shaker* channel from (Chanda *et al.*, 2005). The result of the calculated transmembrane field is shown in Fig. 8. As expected, it is observed that the transmembrane field across the voltage sensor is focused. Summing over all partial charges of the *Shaker* channel yielded a gating charge of about 12 to 14 elementary charges, in good accord with experiments (Schoppa *et al.*, 1992). As shown in Fig. 9 the dominant contributions comes from arginine residues in the S4, in accord with experiment (Aggarwal and MacKinnon, 1996; Seoh *et al.*, 1996). While this calculation is based on approximate structural models (Chanda *et al.*, 2005), it helps illustrate that the observed gating charge

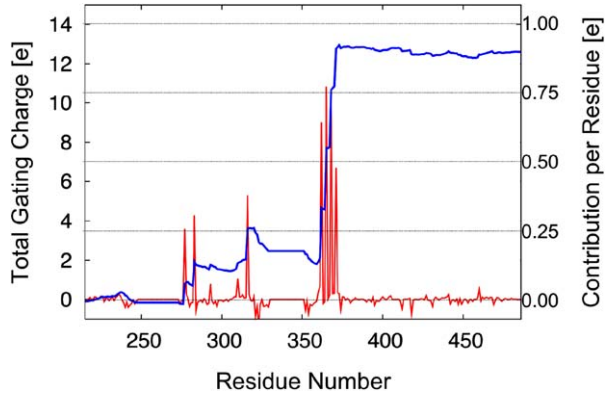

FIGURE 9 Computation of the gating charge from the approximate models of (Chanda *et al.*, 2005) using the PB-V equation (Roux, 1997). The cumulative gating charge (left axis) is shown in blue and the contributions from the individual residues (right axis) is shown in red. (For interpretation of the references to color in this figure legend, the reader is referred to the web version of this book.)

can, in principle, be reproduced without a full translocation of S4 across the bilayer.

IV. CONCLUSION

The progress in understanding the mechanism of voltage-gated channels in recent years has been remarkable. In many ways, there remains much to be done. Even the available X-ray structure of the Kv1.2 channel, which represents a remarkable achievement, is only of moderate resolution and several important regions of the protein are poorly defined (Long *et al.*, 2005). There is currently no atomic resolution structure of the closed state. All we have are approximate models generated from a wide range of data (Chanda *et al.*, 2005; Yarov-Yarovoy et al., 2006; Campos *et al.*, 2007; Pathak *et al.*, 2007; Tombola *et al.*, 2007). While there is little doubt that those models are qualitatively correct, they do not provide the sufficient atomic resolution that is required for detailed quantitative computations. Furthermore, there are probably a number of intermediate states, which will need to be characterized to reach a complete understanding of the mechanism (Bezanilla *et al.*, 1994; Zagotta *et al.*, 1994; Ledwell and Aldrich, 1999). More efforts will also be needed to better characterize the membrane environment of the protein. For example, recent experimental results indicated that the channel does not function well in membranes that formed by lipids that lack the phospho-di-ester group (Schmidt *et al.*, 2006). In the years to come, it can be anticipated that structural modeling and molecular dynamics simulations based on detailed models will continue to contribute to the progress in this exciting field.

Acknowledgements

This work was supported by grants form the National Institute of Health GM62342.

References

Aggarwal, S., MacKinnon, R. (1996). Contribution of the S4 segment to gating charge in the Shaker K^+ channel. *Neuron* **16**, 1169–1177.

Bezanilla, F. (2000). The voltage sensor in voltage-dependent ion channels. *Physiol. Rev.* **80**, 555–592.

Bezanilla, F., Perozo, E., Stefani, E. (1994). Gating of Shaker K^+ channels: II. The components of gating currents and a model of channel activation. *Biophys. J.* **66**, 1011–1021.

Bezanilla, F., Ruta, V., Chen, J., Lee, A., MacKinnon, R. (2003). The principle of gating charge movement in a voltage-dependent K^+ channel. *Nature* **423**, 42–48.

Campos, F.V., Chanda, B., Roux, B., Bezanilla, F. (2007). Two atomic constraints unambiguously position the S4 segment relative to S1 and S2 segments in the closed state of Shaker K channel. *Proc. Natl. Acad. Sci. USA* **104** (19), 7904–7909.

Catterall, W.A. (1988). Structure and function of voltage-sensitive ion channels. *Science* **242**, 50–61.

Cha, A., Snyder, G., Selvin, P., Bezanilla, F. (1999). Atomic scale movement of the voltage-sensing region in a potassium channel measured via spectroscopy. *Nature* **402**, 809–813.

Chanda, B., Asamoah, O.K., Blunck, R., Roux, B., Bezanilla, F. (2005). Gating charge displacement in voltage-gated ion channels involves limited transmembrane movement. *Nature* **436**, 852–856.

Cohen, B.E., Grabe, M., Jan, L.Y. (2003). Answers and questions from the KvAP structures. *Neuron* **39**, 395–400.

Cuello, L., Cortes, D., Perozo, E. (2004). Molecular architecture of the KvAP voltage-dependent K^+ channel in a lipid bilayer. *Science* **306**, 491–495.

Dorairaj, S.J., Allen, T.W. (2007). On the thermodynamic stability of a charged arginine side chain in a transmembrane helix. *Proc. Natl. Acad. Sci. USA* **104** (12), 4943–4948.

Grabe, M., Lecar, H., Jan, Y.N., Jan, L.Y. (2004). A quantitative assessment of models for voltage-dependent gating of ion channels. *Proc. Natl. Acad. Sci. USA* **101**, 17640–17645.

Hille, B. (2001). "Ion Channels of Excitable Membranes", 3rd ed. Sinauer, Sunderland, MA.

Islas, L.D., Sigworth, F.J. (2001). Electrostatics and the gating pore of Shaker potassium channels. *J. Gen. Physiol.* **117**, 69–89.

Jiang, Y., Lee, A., Chen, J., Cadene, M., Chait, B.T., MacKinnon, R. (2002). Crystal structure and mechanism of a calcium-gated potassium channel. *Nature* **417**, 515–522.

Jiang, Y., Lee, A., Chen, J., Ruta, V., Cadene, M., Chait, B., MacKinnon, R. (2003a). X-ray structure of a voltage-dependent K^+ channel. *Nature* **423**, 33–41.

Jiang, Y., Ruta, V., Chen, J., Lee, A., MacKinnon, R. (2003b). The principle of gating charge movement in a voltage-dependent K^+ channel. *Nature* **423**, 42–48.

Jogini, V., Roux, B. (2007). Dynamics of the Kv1.2 voltage-gated K^+ channel in a membrane environment. *Biophys. J.* **93** (9), 3070–3082.

Laine, M., Lin, M.C.A., Bannister, J.P.A., Silverman, W.R., Mock, A.F., Roux, B., Papazian, D.M. (2003). Atomic proximity between S4 segment and pore domain in Shaker potassium channels. *Neuron* **39**, 467–481.

Laine, M., Papazian, D.M., Roux, B. (2004). Critical assessment of a proposed model of Shaker. *FEBS Lett.* **564**, 257–263.

Ledwell, J.L., Aldrich, R.W. (1999). Mutations in the S4 region isolate the final voltage-dependent cooperative step in potassium channel activation. *J. Gen. Physiol.* **113**, 389–414.

Long, S.B., Campbell, E.B., MacKinnon, R. (2005). Crystal structure of a mammalian voltage-dependent Shaker family K^+ channel. *Science* **309**, 897–903.

Lu, Z., Klem, A., Ramu, Y. (2001). Ion conduction pore is conserved among potassium channels. *Nature* **413**, 809–813.

Murata, T., Yamato, I., Kakinuma, Y., Leslie, A.G.W., Walker, J.E. (2005). Structure of the rotor of the V-type Na-ATPase from enterococcus hirae. *Science* **308**, 654–659.

Okamura, Y., Murata, Y., Iwasaki, H., Sasaki, M. (2006). [New role of voltage sensor: Voltage-regulated phosphatase recently identified from ascidian genome]. *Tanpakushitsu Kakusan Koso* **51**, 18–26.

Papazian, D.M., Timpe, L.C., Jan, Y.N., Jan, L.Y. (1991). Alteration of voltage-dependence of Shaker potassium channel by mutations in the S4 sequence. *Nature* **349**, 305–310.

Pathak, M.M., Yarov-Yarovoy, V., Agarwal, G., Roux, B., Barth, P., Kohout, S., Tombola, F., Isacoff, E.Y. (2007). Closing in on the resting state of the Shaker K(+) channel. *Neuron* **56** (1), 124–140.

Phillips, L.R., Milescu, M., Li-Smerin, Y., Mindell, J.A., Kim, J.I., Swartz, K.J. (2005). Voltage-sensor activation with a tarantula toxin as cargo. *Nature* **436**, 857–860.

Posson, D.J., Ge, P., Miller, C., Bezanilla, F., Selvin, P.R. (2005). Small vertical movement of a K^+ channel voltage sensor measured with luminescence energy transfer. *Nature* **436**, 848–851.

Ramsey, I.S., Moran, M.M., Chong, J.A., Clapham, D.E. (2006). A voltage-gated proton-selective channel lacking the pore domain. *Nature* **440**, 1213–1216.

Roux, B. (1997). The influence of the membrane potential on the free energy of an intrinsic protein. *Biophys. J.* **73**, 2980–2989.

Roux, B., Simonson, T. (1999). Implicit solvent models. *Biophys. Chem.* **78**, 1–20.

Ruta, V., Chen, J., MacKinnon, R. (2005). Calibrated measurement of gating-charge arginine displacement in the KvAP voltage-dependent K^+ channel. *Cell.* **123**, 463–475.

Schmidt, D., Jiang, Q.X., MacKinnon, R. (2006). Phospholipids and the origin of cationic gating charges in voltage sensors. *Nature* **444**, 775–779.

Schoppa, N.E., McCormack, K., Tanouye, M.A., Sigworth, F.J. (1992). The size of gating charge in wild-type and mutant Shaker potassium channels. *Science* **255**, 1712–1715.

Selvin, P.R. (2002). Principles and biophysical applications of lanthanide-based probes. *Ann. Rev. Biophys. Biomol. Struct.* **31**, 275–302.

Seoh, S., Sigg, D., Papazian, D., Bezanilla, F. (1996). Voltage-sensing residues in the S2 and S4 segments of the Shaker K^+ channel. *Neuron* **16**, 1159–1167.

Sigworth, F.J. (1993). Voltage gating of ion channels. *Quat. Rev. Biophys.* **27**, 1–40.

Starace, D., Bezanilla, F. (2004). A proton pore in a potassium channel voltage sensor reveals a focused electric field. *Nature* **427**, 548–553.

Tempel, B.L., Papazian, D.M., Schwarz, T.L., Jan, Y.N., Jan, L.Y. (1987). Sequence of a probable potassium channel component encoded at Shaker locus of Drosophila. *Science* **237**, 770–775.

Tombola, F., Pathak, M.M., Gorostiza, P., Isacoff, E.Y. (2007). The twisted ion-permeation pathway of a resting voltage-sensing domain. *Nature* **445**, 546–549.

Tombola, F., Pathak, M.M., Isacoff, E.Y. (2005). Voltage-sensing arginines in a potassium channel permeate and occlude cation-selective pores. *Neuron* **45**, 379–388.

Treptow, W., Tarek, M. (2006). Environment of the gating charges in the Kv1.2 Shaker potassium channel. *Biophys. J.* **90**, L64–L66.

Yarov-Yarovoy, V., Baker, D., Catterall, W.A. (2006). Voltage sensor conformations in the open and closed states in ROSETTA structural models of K(+) channels. *Proc. Natl. Acad. Sci. USA* **103**, 7292–7297.

Yellen, G. (1998). The moving parts of voltage-gated ion channels. *Quant. Rev. Biophys.* **31**, 239–295.

Zagotta, W.N., Hoshi, T., Aldrich, R.W. (1994). Shaker potassium channel gating. III: Evaluation of kinetic models for activation. *J. Gen. Physiol.* **103**, 321–362.